two mechanisms causing surface roughening and surface haze, namely, (1) extrusion haze, which results from flow disturbances at the die exit caused by the elastic nature of the polymer melt, and (2) crystallization haze, which results from stress-induced crystallization close to the film surface.

To obtain low-haze film it is necessary to reduce both extrusion haze and crystallization haze. Extrusion haze can be reduced by selecting polymers which contain a relatively low concentration of large molecules and by intensive mechanical deformation of the melt prior to film extrusion. Mechanical treatment reduces elasticity and film haze by a reversible physical mechanism that generates a long-lived nonequilibrium melt structure, rather than by a chemical mechanism involving chain cleavage and cross-linking. The relaxation time toward the equilibrium melt structure is long compared to typical residence times in extrusion equipment, so the benefits of reduced melt elasticity obtained by mechanical treatment can be realized in practical processing operations such as the film-blowing process. The effect of mechanical treatment must also be considered in developing correlations between polymer chain structure and physical properties.

The detailed mechanism by which crystallization causes surface roughening is not so well understood, and methods for reducing crystallization haze are not so apparent. However, increasing the structural irregularity of the polymer chains probably reduces crystallization-caused surface roughening, and it probably also reduces internal haze to yet lower levels.

References and Notes

(1) Stein, R. S. In "Structure and Properties of Polymer Films"; Lenz, R. W., Stein, R. S., Eds.; Plenum Press: New York, 1973; p 1.
(2) Hashimoto, T.; Todo, A.; Murakimi, Y.; Kawei, H. *J. Polym. Sci., Polym. Phys. Ed.* **1977**, *15*, 501.
(3) Huck, N. D.; Clegg, P. L. *SPE Trans.* **1961**, *1*, 121.
(4) Perron, P. J.; Lederman, P. D. *Polym. Eng. Sci.* **1972**, *12*, 340.
(5) Fujiki, T. *J. Appl. Polym. Sci.* **1971**, *15*, 47.
(6) Foster, G. N. *Polym. Prepr., Am. Chem. Soc., Div. Polym. Chem.* **1979**, *20*, 463.
(7) Shroff, R. N.; Cancio, L. V.; Shida, M. *Polym. Eng. Sci.* **1977**, *17*, 796.
(8) Albright, L. F. *Chem. Eng. (N.Y.)* **1966**, *73*, 113.
(9) Howells, E. R.; Benbow, J. J. *Trans. J. Plast. Inst.* **1962**, *30*, 240.
(10) Rokudai, M. *J. Appl. Polym. Sci.* **1979**, *23*, 463.
(11) Prichard, J. H.; Wissbrun, K. F. *J. Appl. Polym. Sci.* **1969**, *13*, 233.
(12) Hanson, D. F. *Polym. Eng. Sci.* **1969**, *9*, 405.
(13) Drott, E. E.; Mendelson, R. A. *J. Polym. Sci., Part A-2* **1970**, *8*, 1361.
(14) Westerman, L.; Clark, J. C. *J. Polym. Sci., Polym. Phys. Ed.* **1973**, *11*, 559.
(15) Chung, C. I.; Clark, J. C.; Westerman, L. In "Advances in Polymer Science and Engineering"; Pae, K. D., Morrow, D. R., Chen, Yu, Eds.; Plenum Press: New York, 1972; p 249.
(16) Stein, R. S.; Rhodes, M. B. *J. Appl. Phys.* **1960**, *31*, 1873.
(17) Peterlin, A. *Polym. Prepr., Am. Chem. Soc., Div. Polym. Chem.* **1975**, *16*, 315.
(18) Rokudai, M.; Fujiki, T. *J. Appl. Polym. Sci.* **1979**, *23*, 3295.
(19) Bagley, E. B.; Schreiber, H. P. In "Rheology"; Eirich, F. R., Ed.; Academic Press: New York, 1969; Vol. 5, p 93.
(20) Rhodes, M. B.; Stein, R. S. *J. Polym. Sci.* **1960**, *45*, 521.
(21) Nagasawa, T.; Matsumura, T.; Hoshio, S. *Appl. Polym. Symp.* **1973**, *20*, 295.
(22) Spruiell, J. E.; White J. L. *Polym. Eng. Sci.* **1975**, *15*, 660.
(23) Dahl, A. I., Ed. "Temperature, Its Measurement and Control in Science and Industry"; Reinhold: New York, 1962; Vol. 3, Part 2, p 381.
(24) Mandelkern, L.; Maxfield, J. *J. Polym. Sci., Polym. Phys. Ed.* **1979**, *17*, 1913.

Dynamic Small-Angle X-ray Scattering Studies on Diffusion of Macromolecules in Bulk. 2. Principle and Preliminary Experimental Results†

Takeji Hashimoto,* Yasuhisa Tsukahara,‡ and Hiromichi Kawai

Department of Polymer Chemistry, Faculty of Engineering, Kyoto University, Kyoto 606, Japan.

Received October 2, 1980

ABSTRACT: We discuss the change in X-ray, light, and neutron elastic scattering intensity distributions with time when phase-separated structures in block polymers or polymer blends are transformed into a homogeneous mixture by suddenly removing the thermodynamic driving force for the phase separation, e.g., by a temperature jump. During the phase separation the intensity decays exponentially with time at a rate depending on a diffusion coefficient D_c for the center-of-mass motion of the molecules in bulk and q^2, where $q = (4\pi/\lambda) \sin(\theta/2)$ is the scattering vector, which provides a possible approach for evaluating D_c for the self-diffusion. As an application, we evaluated the activation energy (13 kcal/mol) for the diffusion of a particular block polymer of styrene and isoprene by the small-angle X-ray scattering technique, the result of which is consistent with values estimated from rheological measurements.

I. Introduction

Rheological properties of bulk polymers in melts are greatly affected by the molecular entanglements in the system because the entanglements affect the molecular motion.[1] Studies on the translational diffusion of polymer molecules in bulk would be especially of value and provide important information on the physics of entangled systems.[1-3] For example, a classical entanglement-coupling model proposed by Bueche[4] predicts the translational diffusion coefficient D_c for the center-of-mass motion of polymer molecules in bulk to be given by

$$D_c \propto M^{-3.5}$$

† Part 1 of this series corresponds to ref 17.
‡ Present address: Department of Synthetic Chemistry, Faculty of Engineering, Nagoya University, Nagoya 464, Japan.

0024-9297/81/2214-0708$01.25/0

where M is the molecular weight of the polymer. On the other hand, the new concept of "reptation" proposed by de Gennes[5] on the translation diffusion of long molecules in the entangled melts predicts

$$D_c \propto M^{-2}$$

The translational diffusion coefficients have been measured for various polymer systems by a number of techniques such as (i) the radioactive labeling technique,[4,6-8] where one measures the rate of penetration of labeled molecules from one part of the polymer matrix to another matrix which does not originally contain the labeled molecule, (ii) the NMR spin-echo technique,[9-13] associated with the translational diffusion of nuclear magnetic spin due to translational diffusion of the center-of-mass of the molecule as a whole, and (iii) the infrared microdensitometry technique,[14] where, as in technique i, one measures the diffusion broadening in the spatial distribution of the diffusant labeled for IR radiation; i.e., the diffusant has some functional groups which strongly absorb IR radiation at a labeling frequency where there is little absorption by the polymer matrix. Klein and Briscoe[14] have recently experimentally verified the relationship $D_c \propto M^{-2}$ and supported the reptation model for diffusion in linear polyethylene melts at 176 °C by the IR labeling technique.

In this paper we shall apply the scattering technique to measure D_c for self-diffusion of polymers in bulk. Measurements of the translational diffusion coefficient have been a principal subject of photon-correlation spectroscopy in quasi-elastic light scattering.[15,16] However, the techniques can hardly be applied to the measurements of D_c in bulk polymers since the motion is generally too slow. Therefore we are concerned rather with changes of the elastic scattering intensity profile (of light, neutrons, and X-rays) with time due to translational diffusion.

In our case the self-diffusion of macromolecules in bulk takes place when phase-separated structures in block polymers or polymer blends, composed of A and B polymer molecules, are transformed into a homogeneous mixture by removing the thermodynamic driving force for the phase separation, e.g., by a temperature jump. We shall show that decay of the elastic scattered intensity with time is related to D_c and therefore provides an approach for evaluating the diffusion coefficient accompanying the phase transition. Of course, the translational diffusion of polymer molecules accompanied by the phase transition is itself an important theme with respect to the phase transition in heterophase systems, but yet it may also be important to understand the mechanism of diffusion and therefore the physical properties associated with the dynamics of polymer molecules in an entangled polymer matrix. In our previous paper[17] we presented briefly our ideas and experimental results on SAXS studies of the diffusion involved in the phase transition. Here we will describe them in detail.

II. Theoretical Background

1. Model. Let us first describe our model. Block polymers and polymer blends, composed of A and B polymers, form microdomain and macrodomain structures, respectively, due to phase separation. The driving force for the phase separation is the repulsive interaction between the A and B polymers; like segments are segregated into domains. When the thermodynamic driving force for the phase separation is removed suddenly, by a temperature jump, for example, the self-diffusion of polymer molecules takes place, giving rise to a spatial segmental distribution varying with time. We define $\rho_K(\mathbf{r},t)$ as the spatial segmental distribution of K polymers at time t.

We assume that the self-diffusion of polymer molecules in an entangled melt takes place through reptation,[5] i.e., the essentially one-dimensional curvilinear diffusion of a chain molecule along its own contour, as proposed by de Gennes. As the reptation proceeds, the segments lose their memories with respect to their positions in space, resulting eventually in completely uniform segmental density distribution. Each molecule undergoes Brownian motion independently of others and this process can be described by a random stochastic process. We further simplify our treatment by assuming that the temperature should be sufficiently high, much higher than the critical temperature T_c, that the thermodynamic interaction between A and B units does not make a significant contribution to the center-of-mass motion of the polymer molecules.[34] Here we consider that the systems have upper critical solution temperatures, as in the systems composed of polystyrene (PS) and polyisoprene (PI).

In such a simplified system, the self-diffusion of polymer molecules involved in the phase transition is simply Fickian

$$\partial\rho_K(\mathbf{r},t)/\partial t = D_c \nabla^2\rho_K(\mathbf{r},t) \qquad (K = A \text{ or } B) \quad (1)$$

where D_c is the diffusion coefficient for the center-of-mass of the block polymer molecule as a whole or of K homopolymer in the case of polymer blends. Here we assume D_c is independent of spatial position $\mathbf{r}$. In the case of polymer blends we assume $D_{c,A}$ for the A polymer is nearly equal to $D_{c,B}$ for the B polymer; otherwise, we need a correction term in the diffusion equation.[35] This interaction of the diffusional flow between A and B species is associated with the requirement that the overall segment density must be kept constant in space during the diffusion. This requirement originates from the incompressibility of materials and the resultant interaction with the diffusional flow acts as a resistance to the flow of the species having the larger D_c and enhances the flow of the species having the smaller D_c. Probably we will have to impose the constraint of $D_{c,A} \simeq D_{c,B}$ even for the block polymer in order to justify the simple equation (1).

If the temperature is not sufficiently high, we have to start with a modified diffusion equation which contains an extra term to take into account the excess chemical potential of a given species due to thermodynamic interactions between A and B units. However, even if the temperature is not sufficiently high, eq 1 should still be a good approximation for the initial stage of the diffusion, since the range Λ_{AB} involving the thermodynamic interaction is small compared with the ranges of Λ_{AA} and Λ_{BB} involving the hydrodynamic interactions only at the initial stage.

2. One-Dimensional Diffusion. As the simplest case we consider here the diffusion across flat interfaces as in the diffusion in alternating lamellar microdomains of block polymers or in the lamellar-type phase-separated domain in polymer blends. Figure 1 shows that cylindrical coordinates (x,ζ,ϕ) of the system, where the x axis is normal to the flat interface, the yOz plane. The segment density of K polymer at the plane x and at time t, $\rho_K(x,t)$ is given by

$$\rho_K(x,t) = \int\int d\phi\ \zeta\ d\zeta\ \rho_K(x,\zeta,\phi;t) \qquad (K = A \text{ or } B) \quad (2)$$

$\rho_K(x,t)$ also satisfies the diffusion equation

$$\partial\rho_K(x,t)/\partial t = D_c(\partial^2\rho_K(x,t)/\partial x^2) \qquad (K = A \text{ or } B) \quad (3)$$

The one-dimensional diffusion equation should be solved under an appropriate initial condition.

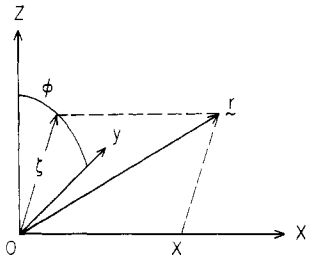

Figure 1. Cylindrical coordinates (x,ζ,ϕ), where x is normal to the flat interface of the lamellar microdomain.

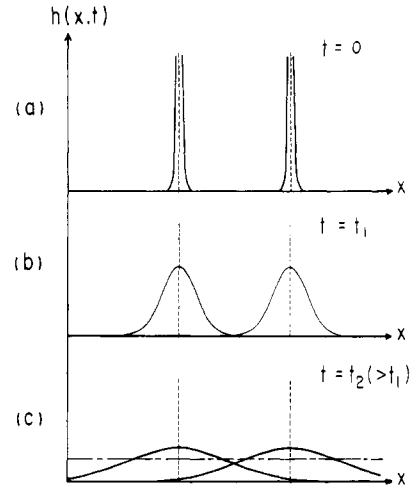

Figure 2. Variation of the function $h(x,t)$ describing diffusion of chemical junction points of block polymers across the interface with time after the T-jump: (a) initial stage; (b) intermediate stage; (c) final stage. Note that $h(x,t)$ corresponds to the spatial distribution of the center of mass of the molecules in the case of polymer blends.

We first consider the diffusion in alternating lamellar microdomains. In the initial microdomain structure, the chemical junction points of the block polymers are restricted to the narrow interfacial region with a characteristic interfacial thickness of about 2.0 nm[19-21] so that its spatial distribution $h(x,t)$ is narrow around the interfaces as in Figure 2a. As self-diffusion takes place, the spatial distribution becomes broader, as in Figure 2b, resulting eventually in a uniform distribution as shown by the dash-dot line in Figure 2c. The spatial distribution $h(x,t)$ should also satisfy diffusion eq 3

$$\partial h(x,t)/\partial t = D_c(\partial^2 h(x,t)/\partial x^2) \tag{4}$$

Accompanying the self-diffusion, the segmental density profile also changes with time as shown in Figure 3. Initially there are regions composed of pure A (i.e., the region having $\tilde{\rho}_A = 1$, $\tilde{\rho}_A$ being the segment density in the domain space relative to that of bulk A) or B, if the repulsive interaction is sufficiently high, as in polystyrene-polyisoprene (SI) block polymers. As the self-diffusion takes place, the interfacial thickness ξ increases and the mixing of A and B segments proceeds as shown in the intermediate stage (Figure 3b), eventually resulting in a completely uniform segmental density distribution (dash-dot line of Figure 3c).

If the initial segment density pattern $\tilde{\rho}_K(x,t = 0)$ is given by a periodic function with a repeat distance $2l$, having domain sizes $2a$ and $2l - 2a$ for the A and B domains, respectively, and a sharp boundary with infinitesimal interfacial thickness between the two coexisting phases A and B, i.e., $\xi = 0$, then

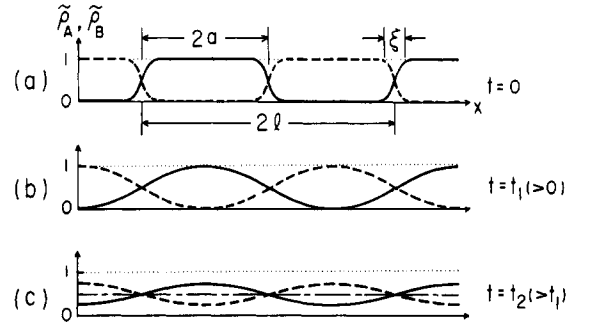

Figure 3. Variation of the segmental density profile of block copolymers and polymer blends with time after the T-jump: (a) initial stage; (b) intermediate stage; (c) final stage. $\tilde{\rho}_K$ is the segment density relative to that of bulk K. Note in the case of polymer blends $\tilde{\rho}_K$ is not necessarily periodic.

$$\tilde{\rho}_A(x,t = 0) = \rho_A(x,t = 0)/\rho_{A0} = \frac{a}{l} + \frac{2}{\pi}\sum_{m=1}^{\infty}\frac{1}{m}\sin\left(\frac{m\pi a}{l}\right)\cos\left(\frac{m\pi x}{l}\right) \tag{5}$$

and

$$\tilde{\rho}_B(x,t = 0) = \frac{a}{l} + \frac{2}{\pi}\sum_{m=1}^{\infty}\frac{1}{m}\sin\left(\frac{m\pi a}{l}\right)\cos\left(\frac{m\pi(x - 2a)}{l}\right) \tag{6}$$

where ρ_{K0} is the number density of the K segment in the homopolymer K.

From eq 3 and 5, the segment density ρ_A at time t is given by[22]

$$\tilde{\rho}_A(x,t) = \frac{a}{l} + \frac{2}{\pi}\sum_{m=1}^{\infty}\exp\left(-\frac{m^2\pi^2 D_c}{l^2}t\right)\frac{1}{m}\sin\left(\frac{m\pi a}{l}\right)\cos\left(\frac{m\pi x}{l}\right) \tag{7}$$

$\tilde{\rho}_A(x,t)$ is rewritten as

$$\tilde{\rho}_A(x,t) = \tilde{\rho}_A(x,t = 0) * h(x,t) \tag{8}$$

where $h(x,t)$ is given by

$$h(x,t) = (2\pi\sigma_1^2)^{-1/2}\exp(-x^2/2\sigma_1^2) \qquad \sigma_1^2 = 2D_c t \tag{9}$$

The asterisk designates a convolution operation

$$f * g(x) = \int du\, f(u)g(x - u) \tag{10}$$

It should be noted that the function $h(x,t)$ represents the spatial distribution of the chemical junction points and is a solution of eq 4 with the initial condition of a sharp boundary

$$h(x,t = 0) = \delta(x) \tag{11}$$

If the domain structure has a diffuse boundary at $t = 0$, the initial condition (11) should be replaced by a Gaussian function

$$h(x,t = 0) \equiv h_{01}(x) = (2\pi\sigma_{01}^2)^{-1/2}\exp(-x^2/2\sigma_{01}^2) \tag{12}$$

where σ_{01} is a parameter characterizing the interfacial thickness at time $t = 0$. In this case, a solution of eq 4 (which is designated as $h_1(x,t)$) is given by

$$h_1(x,t) = h_{01}(x) * h(x,t) = [2\pi(\sigma_{01}^2 + \sigma_1^2)]^{-1/2}\exp[-x^2/2(\sigma_{01}^2 + \sigma_1^2)] \tag{13}$$

where σ_1 is given by eq 9. Equation 13 is a generalized

form of eq 9, and the corresponding segmental density distribution $\rho_K(x,t)$ is given by

$$\tilde{\rho}_K(x,t) = \tilde{\rho}_K(x,t=0) * h_1(x,t) \quad (14)$$

Although eq 13 and 14 are derived for phase-separated systems with a periodic segmental density distribution, the equations are obviously valid for any phase-separated system with a nonperiodic density distribution, as is typical in polymer blends, if eq 5 and 6 are replaced by the functions relevant to the nonperiodic systems.

In case of polymer blends, $h(x,t)$ corresponds to the spatial distribution of the center of mass of a given molecule A or B at time t. As in block polymers, the center of mass of the K molecules is rich in the K domain due to the repulsive force between A and B, resulting in the center-of-mass distribution in space shown in Figure 2 (the spatial distribution not necessarily being periodic as in the figure). The spatial distribution of the center-of-mass gives rise to the segmental density distribution as also shown in Figure 3 (again the distribution not necessarily being periodic). Thus the problem in polymer blends is identical with that of block polymers (if $D_{c,A} \simeq D_{c,B}$, as discussed already).

3. Two- and Three-Dimensional Diffusion. The treatment in the preceding section can readily be generalized into two- or three-dimensional diffusion as encountered in systems having spherical or cylindrical domains, respectively. The initial conditions corresponding to eq 12 for the two- and three-dimensional systems are given by, respectively

$$h_{02}(\mathbf{r}) = (\pi\sigma_{02}^2)^{-1} \exp(-r^2/\sigma_{02}^2) \quad (15)$$

and

$$h_{03}(\mathbf{r}) = (3/2\pi\sigma_{03}^2)^{3/2} \exp(-3r^2/2\sigma_{03}^2) \quad (16)$$

The diffusion equation corresponding to eq 4 is given by

$$\partial h(\mathbf{r},t)/\partial t = D_c \nabla^2 h(\mathbf{r},t) \quad (17)$$

and the solutions are given by

$$h_2(\mathbf{r},t) = [\pi(\sigma_{02}^2 + \sigma_2^2)]^{-1} \exp[-r^2/(\sigma_{02}^2 + \sigma_2^2)] \quad (18)$$

$$\sigma_2^2 = 4D_c t \quad (19)$$

for the two-dimensional diffusion process and

$$h_3(\mathbf{r},t) = \left[\frac{3}{2\pi(\sigma_{03}^2 + \sigma_3^2)}\right]^{3/2} \exp\left[\frac{-3r^2}{2(\sigma_{03}^2 + \sigma_3^2)}\right] \quad (20)$$

$$\sigma_3^2 = 6D_c t \quad (21)$$

for the three-dimensional diffusion process. The corresponding segmental density patterns $\tilde{\rho}_{K,j}(\mathbf{r},t)$ for K polymer are then given by

$$\tilde{\rho}_{K,j}(\mathbf{r},t) = \tilde{\rho}_{K,j}(\mathbf{r},t=0) * h_j(\mathbf{r},t) \qquad (K = A \text{ or } B) \quad (22)$$

where j denotes the dimensionality ($j = 1, 2, 3$). $\tilde{\rho}_{K,j}(r,t=0)$ is the initial segmental density pattern which is either periodic or nonperiodic.

4. Elastic Scattering Behavior. We can calculate the electron density distribution $\rho_e(\mathbf{r},t)$, the quantity necessary to calculate the X-ray scattering, at time t from the segment density profile $\tilde{\rho}_K(x,t)$

$$\rho_e(\mathbf{r},t) = n_A\rho_A(\mathbf{r},t) + n_B\rho_B(\mathbf{r},t) \quad (23)$$

where n_K is the number of electrons per segment for a K-type polymer. n_K corresponds to the polarizability and scattering length per segment for light and neutron scattering, respectively. Since

$$\rho_K(\mathbf{r},t) = \rho_{0K}\tilde{\rho}_{K,j}(\mathbf{r},t) = \rho_{K,j}(\mathbf{r},t=0) * h_j(\mathbf{r},t) \quad (24)$$

it follows that

$$\rho_e(\mathbf{r},t) = \rho_e(\mathbf{r},t=0) * h_j(\mathbf{r},t) \quad (25)$$

where

$$\rho_e(\mathbf{r},t=0) = n_A\rho_{A,j}(\mathbf{r},t=0) + n_B\rho_{B,j}(\mathbf{r},t=0) \quad (26)$$

the initial contrast distribution.

The amplitude $E(q,t)$ and intensity $I(q,t)$ of the scattered X-rays, light, and neutrons from the systems are given by

$$E(q,t) = \mathcal{F}\{\rho_e(\mathbf{r},t)\} = \mathcal{F}\{\rho_e(\mathbf{r},t=0)\}\mathcal{F}\{h_j(\mathbf{r},t)\} \quad (27)$$

and

$$I(q,t) = \mathcal{I}(q,t=0)|\mathcal{F}\{h_j(\mathbf{r},t)\}|^2 \quad (28)$$

where $\mathcal{I}(q,t=0) = |\mathcal{F}\{\rho_e(\mathbf{r},t=0)\}|^2$ is the fictitious scattered intensity at $t = 0$ that the system would have if the interfacial thickness of the system were zero; i.e., $\sigma_{0j} = 0$ at $t = 0$. $\mathcal{F}\{\rho_e\}$ denotes the Fourier transform of the function ρ_e

$$\mathcal{F}\{\rho_e(\mathbf{r},t)\} = \int d\mathbf{r}\, \rho_e(\mathbf{r},t) \exp[i(\mathbf{q}\cdot\mathbf{r})] \quad (29)$$

In eq 27 and 28, we assume the system is isotropic so that E and I depend only on the magnitude of the scattering vector $\mathbf{q}$

$$|\mathbf{q}| = (4\pi/\lambda) \sin(\theta/2) \quad (30)$$

where λ is the wavelength in the medium and θ is the scattering angle.

Now from eq 13 and 18–21, it follows that

$$\mathcal{F}\{h_j(\mathbf{r},t)\} = \exp[-(\sigma_{0j}^2 + \sigma_j^2)q^2/2j] \quad (31)$$

$$\sigma_j^2 = 2jD_c t \qquad j = 1, 2, 3 \quad (32)$$

If we define the parameter σ_0 associated with the initial interfacial thickness as

$$\sigma_{0j}^2 \equiv j\sigma_0^2 \quad (33)$$

then eq 31 is rewritten by

$$\mathcal{F}\{h_j(\mathbf{r},t)\} = \exp[-(\sigma_0^2 + 2D_c t)q^2/2] \quad (34)$$

irrespective of i, the dimensionality. Consequently, it follows that

$$I(q,t) = \mathcal{I}(q,t=0) \exp[-(\sigma_0^2 + 2D_c t)q^2] \quad (35)$$

$$I(q,t) = I(q,t=0) \exp(-2q^2D_c t) \quad (36)$$

or

$$\ln[I(q,t)/I(q,t=0)] = -2q^2D_c t \quad (37)$$

where

$$I(q,t=0) = \mathcal{I}(q,t=0) \exp(-\sigma_0^2q^2) \quad (38)$$

i.e., the scattering intensity at time $t = 0$. Equations 36 and 37 are valid, irrespective of the dimensionality and the periodicity (all the information is included in the initial intensity profile $I(q,t=0)$), as long as the self-diffusion can be described as Fickian. Thus the intensity decays exponentially with time at a rate which depends on D_c and q^2.[34,35]

5. Growth of Interfacial Region Accompanying the Phase Transition. The self-diffusion process also predicts a growth of the interfacial thickness during the phase transition. If we define the characteristic interfacial thickness ξ as

$$\xi(t)^{-1} = |d\tilde{\rho}_K(\mathbf{r},t)/dr|_{\tilde{\rho}_K=1/2} \quad (39)$$

$\xi(t)$ is given, from eq 14, 18–22, 33, and 39, by

$$\xi(t) = [2(\sigma_0^2 + 2D_c t)]^{1/2} \tag{40}$$

again irrespective of the dimensionality and the periodicity.

6. Molecular Parameters Affecting D_c. We can relate D_c, the diffusion coefficient for the center-of-mass motion, to the diffusion coefficient for the reptation, D_r. By imposing a random walk configuration on an essentially one-dimensional curvilinear diffusion of polymer molecules along its own contour, one obtains[23,24]

$$D_c = (\langle R^2\rangle/3\langle L^2\rangle)D_r \tag{41}$$

where $\langle R^2\rangle$ and $\langle L^2\rangle$ are the mean-square end-to-end distance and contour length of the polymer chain, respectively.

Now according to Einstein's relation for the fluctuation–dissipation theorem, D_r is given for an A–B-type diblock polymer by

$$D_r = k_B T/(\mathcal{L}_{r,A}Z_A + \mathcal{L}_{r,B}Z_B) \tag{42}$$

where k_B is the Boltzmann constant, Z_K is the degree of polymerization for a K polymer, and $\mathcal{L}_{r,K}$ is the monomeric frictional coefficient for the reptation of a K polymer. In general $\mathcal{L}_{r,K}$ should be smaller than the monomeric frictional coefficient of Rouse–Zimm-type motion, $\mathcal{L}_{RZ,K}$.

The temperature dependence of D_c is determined by those of $\mathcal{L}_{r,A}$ and $\mathcal{L}_{r,B}$ and therefore by the activation energies for the respective diffusional processes. Since $\langle R^2\rangle/\langle L^2\rangle \sim Z^{-1}$, D_c is inversely proportional to Z^{-2}, which determines the molecular weight dependence of D_c.

The monomeric frictional coefficient $\mathcal{L}_{r,A}$ of an A unit may be a weighted average of the frictional coefficients of the A–A interaction ($\mathcal{L}_{r,AA}$) and the A–B interaction ($\mathcal{L}_{r,AB}$)

$$\begin{aligned}\mathcal{L}_{r,A} &= \mathcal{L}_{r,AA}\phi_A + \mathcal{L}_{r,AB}(1-\phi_A)\\ \mathcal{L}_{r,B} &= \mathcal{L}_{r,BA}(1-\phi_B) + \mathcal{L}_{r,BB}\phi_B\end{aligned} \tag{43}$$

where ϕ_A and ϕ_B are the mole fractions of A chains in the A domain and B chains in the B domain, respectively. At an initial stage of diffusion, $\phi_A \simeq 1$ and $\phi_B \simeq 1$ and therefore

$$\mathcal{L}_{r,A} \simeq \mathcal{L}_{r,AA} \qquad \mathcal{L}_{r,B} \simeq \mathcal{L}_{r,BB} \tag{44}$$

Therefore $\mathcal{L}_{r,A}$ and $\mathcal{L}_{r,B}$ are nearly equal to the monomeric frictional coefficients in the corresponding homopolymers.

III. Experimental Section

1. Materials. We have used a "tapered" block polymer of styrene and isoprene. The polymer was prepared by the simultaneous copolymerization of a mixture of purified styrene and isoprene, containing a trace amount of tetrahydrofuran (THF), with *sec*-butyllithium (*s*-BuLi) in benzene as the polymerization solvent at room temperature. This procedure causes the propagating polymer chain to be rich in isoprene until late in the reaction, after which styrene incorporation increases. A trace amount of THF was added to reduce blockiness in the sequence distribution of the two monomers or to increase the degree of mixing of the two monomers in the primary structure. The polymer has a total number-average molecular weight of 4.3×10^4, has a heterogeneity index $\bar{M}_w/\bar{M}_n$ of 1.05, and contains 47 wt % styrene; details are given elsewhere.[25] A trace amount of *N*-phenyl-β-naphthylamine was added to the polymer in order to reduce the effect of oxidation during the experiments.

2. Methods. High-speed observation of SAXS profiles accompanying the phase transition was conducted with a dynamic small-angle X-ray scattering apparatus constructed in our laboratory. The apparatus is composed of a 12-kW rotating-anode X-ray generator, a graphite monochromator (Cu Kα radiation), a pair of collimating pinholes or slits, a vacuum chamber, a linear position sensitive proportional counter, position-analyzing electronics, a multichannel analyzer with a 16K-word (16 bits/word) memory area available for scattering data, and a microcomputer for data acquisition, data analysis, and system control. The details will be described elsewhere.[26] The weighting functions along the slit length and slit width are narrow so that the collimation errors do not significantly affect the observed SAXS profiles.

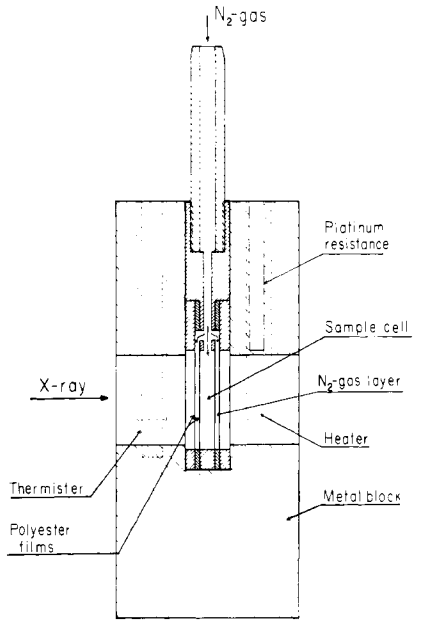

Figure 4. Schematic diagram of a temperature enclosure used for *T*-jump measurements. The sample cell as a whole is rapidly and manually transferred into a metal block which is preheated and controlled at a measuring temperature. The sample is sealed under nitrogen to reduce oxidation.

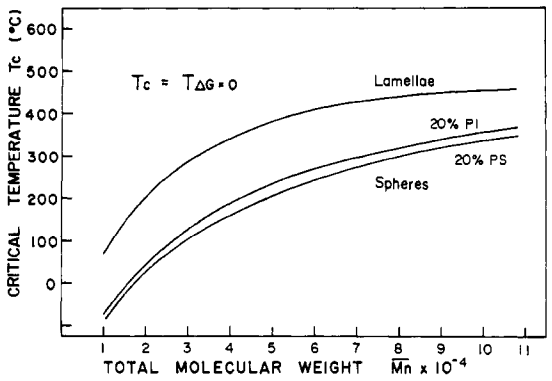

Figure 5. Critical temperature at which the microdomain structure is transformed into a homogeneous mixture. The temperature T_c is calculated from the theory of Helfand–Wasserman based on the narrow interphase approximation for SI-diblock copolymers having lamellar morphology (50 wt % PS) and spherical morphology (20 wt % PS or PI).

The temperature of the specimen was rapidly changed by inserting a sample cell having a relatively small heat capacity into a metal block (having a large heat capacity) preheated and controlled at the measuring temperature. A sample 20-mm high × 4-mm wide × 2.5-mm thick was put into the sample cell and sealed under nitrogen, as shown in Figure 4, to minimize the effect of oxidation. The temperature of the sample was measured by embedding the thermocouple in the sample, the temperature variation with time being sigmoidal and the time required to reach the measuring temperature about 40 s.

IV. Results and Discussion

Ideal block copolymers of polystyrene–polyisoprene (SI) which are prepared by sequential polymerization rather than by simultaneous polymerization generally have a high critical temperature T_c. Figure 5 shows the critical temperatures as a function of total molecular weight of the SI diblock polymers as predicted from Helfand's theory based

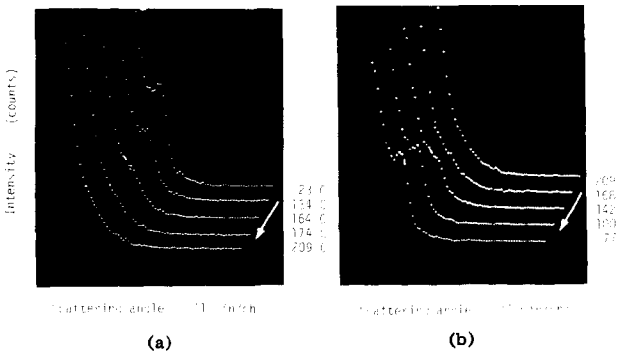

(a) (b)

Figure 6. Typical oscilloscope traces showing the change of the SAXS profile with temperature during the (a) heating and (b) cooling cycles of the tapered block polymer. Each curve was obtained with a 40-s X-ray exposure and shifted diagonally to avoid overlap. The abscissa corresponds to channel number, one channel being 1′ in scattering angle (λ = 1.54 Å). The ordinate corresponds to the number of photons falling on each channel.

on the narrow-interphase approximation.[27] The temperatures T_c were calculated for the lamellar microdomain systems (having a weight fraction of polystyrene (PS) of 0.5) and for the spherical microdomain systems (having weight fractions of PS of 0.2 and 0.8). The molecular parameters required to calculate T_c are given elsewhere.[20,21,28]

Thus ideal block copolymer having a total molecular weight of 4.3×10^4 (corresponding to the tapered block polymer) will have $T_c \simeq 360$ °C, an extremely high temperature. Experimentally this temperature was shown to be higher than 220 °C.[25] As a possible approach to lower T_c without lowering the molecular weight, we consider the tapered block polymer, a special block polymer in which the incompatible units are partially mixed in a given molecule with a tapered composition.

Figure 6 shows typical changes of the SAXS profiles with temperature during (a) heating (4 °C/min) and (b) cooling (2 °C/min) of the tapered block copolymer. Each curve was obtained with 40-s exposure to X-ray radiation and the origin of the curves is shifted diagonally to avoid overlap. The abscissa corresponds to the channel numbers of the multichannel analyzer, one channel corresponding to 1′ in scattering angle. The ordinate corresponds to the number of photons which fall on each channel and therefore to the relative scattered X-ray intensity.

It should be noted that the scattering maximum corresponding to the long-identity period of the microdomain structure (29.2 nm at room temperature) disappears when the temperature is raised to 170 °C and appears again at the same scattering angle with decreasing temperature. During the heating cycle, the peak intensity decreases and the peak position shifts to larger scattering angles; i.e., the long-identity period decreases. These factors suggest that melting of the phase-separated structure to a homogeneous mixture occurs. When the temperature is raised, an effective repulsive interaction between PS and PI decreases so that PS (PI) chains tend to have some walks in the PI (PS) domains, resulting in a decreased domain identity period and a decreased contrast between the two phases. These tendencies are exactly what are found in the experimental results.

The tapered block copolymer may be considered phenomenologically to be a diblock polymer composed of a styrene-rich block sequence and an isoprene-rich block sequence, to a good approximation. The effective repulsive interaction between the two block sequences is naturally much weaker than that between the pure PI and PS block sequences. This enhances the mixing of the two block

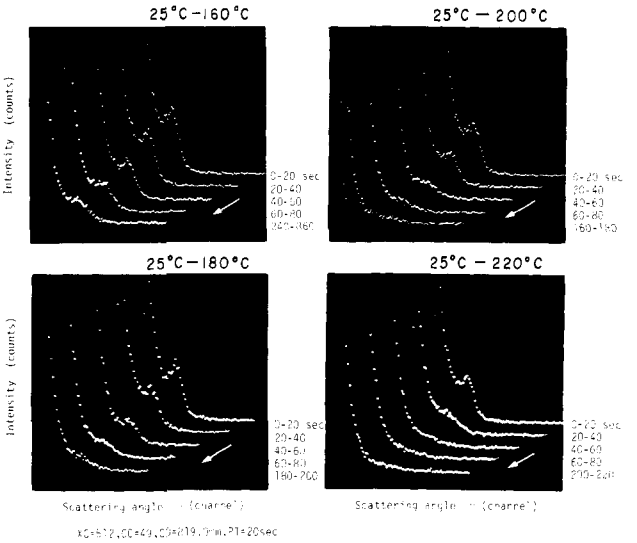

Figure 7. Oscilloscope traces showing the change of the SAXS profile with time after a temperature jump from room temperature to 160, 180, 200, and 220 °C. Each curve was measured with an exposure time of 20 s; one channel corresponds to 1′ in scattering angle.

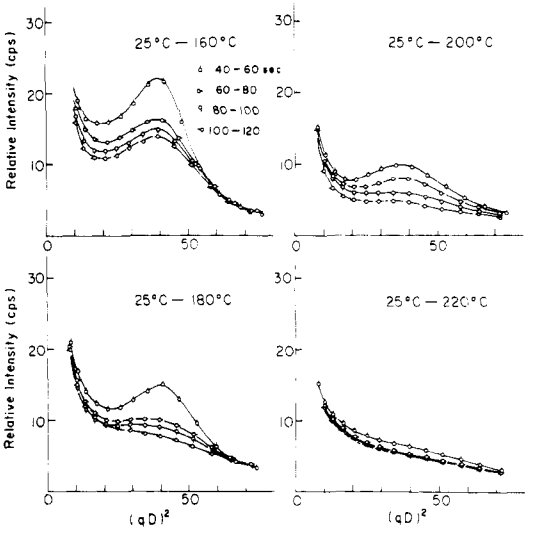

Figure 8. Replot of the data in Figure 7; the intensity is plotted as a function of $(qD)^2$, where q is the scattering vector and D is the long identity period at each temperature.

chains, resulting in a microdomain structure consisting of the polystyrene-rich phase and polyisoprene-rich phase and giving rise to unique dynamic mechanical properties.[25,29] The reduced effective interaction lowers the critical temperature of the tapered block polymer (down to 170 °C) in comparison to that of the ideal block.

Figure 7 demonstrates changes of the SAXS curves with time after a temperature jump from room temperature to 160, 180, 200, and 220 °C, each curve being measured with an exposure of 20 s and each channel corresponding to 1′ in scattering angle. The scattering peak was shown to disappear at a rate which depends upon temperature. In Figure 8 the data are replotted with the intensity as a function of $(qD)^2$, where q is the scattering vector and D is the long-identity period at each temperature.

The decay of the peak intensity with time at a given temperature (in Figure 8) is plotted in Figure 9. From the discussion in section II-4, the slope of the plot yields the diffusion coefficient D_c

$$\mathrm{d} \log [I(t;T,q_{max})]/\mathrm{d}t = -2q_{max}^2 D_c(T)/2.303 \quad (45)$$

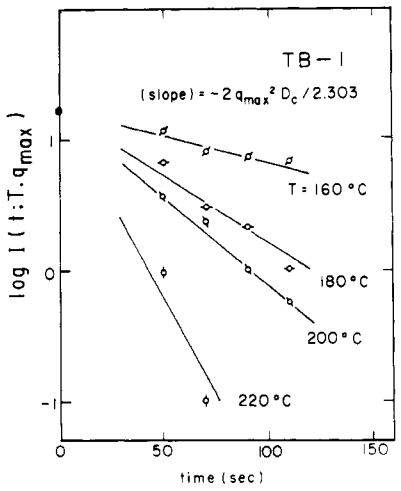

Figure 9. Change of maximum scattered intensity with time after a temperature jump from room temperature to 160, 180, 200, and 220 °C; the slope is related to $D_c(T)$ by eq 45.

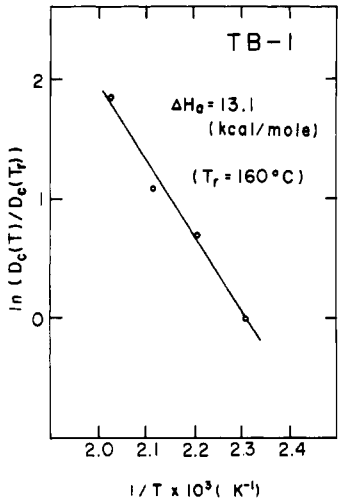

Figure 10. Arrhenius plot for obtaining the activation energy for the translational diffusion of the block polymer in bulk.

The diffusion coefficient thus estimated varies from $\sim 10^{-15}$ to $\sim 10^{-14}$ cm^2/s with increasing temperature from 160 to 220 °C. The effects on the magnitude of D_c of the finite time required to raise the temperature ($\sim$40 s) and the finite measuring time ($\sim$20 s) as well the effect of a measuring temperature below that of the assumption invoked in eq 1 are subjects for further investigation.[30]

We assume the diffusion can be described by an Arrhenius relation

$$D_c(T) = D_c^\circ \exp(-\Delta H_a/RT) \tag{46}$$

where ΔH_a is the activation energy and R is the gas constant. Figure 10 shows the Arrhenius plot, from which ΔH_a = 13.1 kcal/mol is obtained.

If the monomeric friction coefficients for reptation in eq 42 are given by

$$\begin{aligned} \mathcal{L}_{r,A} &= \mathcal{L}_{A0} \exp(\Delta H_A/RT) \\ \mathcal{L}_{r,B} &= \mathcal{L}_{B0} \exp(\Delta H_B/RT) \end{aligned} \tag{47}$$

where ΔH_K is the activation energy for K monomer, then, from eq 41, 42, and 47, the temperature dependence of the diffusion coefficient $D_c(T)$ is given by

$$D_c(T)/D_c^\circ = [w_A e^{\Delta H_A/RT} + w_B e^{\Delta H_B/RT}]^{-1} \tag{48}$$

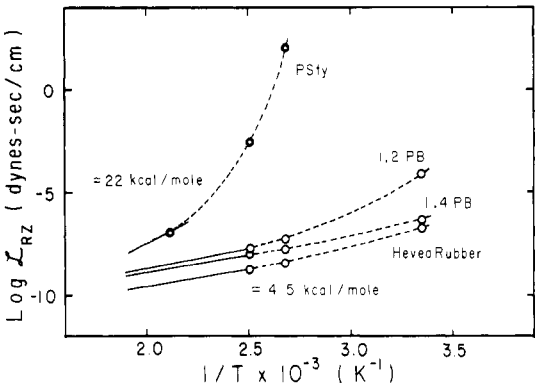

Figure 11. Monomeric friction coefficients (of Rouse–Zimm-type motion) for homo-PS, homo-PB, and homo-PI in bulk as a function of temperature. The data are obtained from Ferry.[1] The activation energies of $\Delta H_{PS} \simeq 22$ and $\Delta H_{PI} \simeq 4$ kcal/mol are obtained for homo-PS and homo-PI for the temperature range of this work, respectively.

Therefore an apparent activation energy for the block polymer ΔH_a is related to ΔH_K (K = A, B)

$$\exp(\Delta H_a/RT) = w_A \exp(\Delta H_A/RT) + w_B \exp(\Delta H_B/RT) \tag{49}$$

where

$$\begin{aligned} w_A &= \mathcal{L}_{A0}Z_A/(\mathcal{L}_{A0}Z_A + \mathcal{L}_{B0}Z_B) \\ w_B &= \mathcal{L}_{B0}Z_B/(\mathcal{L}_{A0}Z_A + \mathcal{L}_{B0}Z_B) \end{aligned} \tag{50}$$

At a very high temperature where $RT > \Delta H_A$, ΔH_B

$$\Delta H_a \simeq w_A \Delta H_A + w_B \Delta H_B \tag{51}$$

If $RT \ll \Delta H_A$, ΔH_B and $\Delta H_A > \Delta H_B$

$$\exp(\Delta H_a/RT) \simeq w_A \exp(\Delta H_A/RT)$$

and therefore

$$\Delta H_a \simeq \Delta H_A \tag{52}$$

The activation energy for the block polymer is nearly equal to that of the block sequence with the higher activation energy.

Figure 11 shows monomeric friction coefficients (of Rouse–Zimm-type motion) for homo-PS, homopolybutadiene (PB), and homo-PI in bulk as a function of $1/T$. The data were obtained from ref 1. Although absolute values of the frictional coefficients for reptation are different from those for Rouse–Zimm type, their activation energies are expected to be essentially identical. In the temperature range of our experiments, $\Delta H_{PS} \simeq 22$ kcal/mol, $\Delta H_{PI} \simeq 4$ kcal/mol, and $RT \simeq 1$ kcal/mol. Thus ΔH_a of the block polymer should be nearly equal to ΔH_{PS}, i.e., approximately 22 kcal/mol. The predicted result is greater than the result (13 kcal/mol) obtained by the SAXS method, which requires further investigation. It may be worthwhile to compare the results evaluated from rheological measurements. Gouinlock and Porter[31] and Chung and Lin[32] have reported the activation energy for diffusion to be 17 and 17.4 kcal/mol, respectively, for polystyrene–polybutadiene–polystyrene (SBS) block copolymers of block molecular weights 7000, 43 000, and 7000, respectively. Arnold and Meier[33] obtained 18.1 kcal/mol for the SBS triblock copolymer block molecular weights of 10 000, 50 000, and 10 000. These values estimated from rheological measurements are slightly greater than that from the SAXS measurement.

Acknowledgment. We thank Dr. E. A. DiMarzio, National Bureau of Standards, for a suggestion which

stimulated this work. This work was supported in part by a Grant-in-Aid for Scientific Research (449012) from the Ministry of Education, Japan.

References and Notes

(1) Ferry, J. D. "Viscoelastic Properties of Polymers", 2nd ed.; Wiley: New York, 1970.
(2) Bueche, F. "Physical Properties of Polymers"; Interscience: London, 1962.
(3) de Gennes, P. G. "Scaling Concepts in Polymer Physics"; Cornell University Press: Ithaca, N.Y., 1979.
(4) Bueche, F. *J. Chem. Phys.* **1968**, *48*, 1410.
(5) de Gennes, P. G. *J. Chem. Phys.* **1971**, *55*, 572.
(6) Bueche, F.; Cashin, W. M.; Debye, P. *J. Chem. Phys.* **1952**, *20*, 1956.
(7) Skewis, J. D. *Rubber Chem. Technol.* **1966**, *39*, 217.
(8) Rhee, C.-K.; Ferry, J. D. *J. Appl. Polym. Sci.* **1977**, *21*, 783.
(9) McCall, D. W.; Anderson, E. W.; Huggins, C. M. *J. Chem. Phys.* **1961**, *34*, 804.
(10) McCall, D. W.; Douglass, D. C.; Anderson, E. W. *J. Chem. Phys.* **1959**, *30*, 771. *J. Polym. Sci., Part A* **1963**, *1*, 1709.
(11) Tanner, J. E. *Macromolecules* **1971**, *4*, 738.
(12) Tanner, J. E.; Lin, K.-J.; Anderson, J. E. *Macromolecues* **1971**, *4*, 586.
(13) Cosgrove, T.; Warren, R. F. *Polymer* **1977**, *18*, 255.
(14) Klein, J.; Briscoe, B. J. *Nature (London)* **1975**, *257*, 386. *Polymer* **1976**, *17*, 481.
(15) Chu, B. "Laser Light Scattering"; Academic Press: New York, 1974.
(16) Berne, B. J.; Pecora, R. "Dynamic Light Scattering"; Wiley: New York, 1976.
(17) Hashimoto, T.; Tsukahara, Y.; Kawai, H. *J. Polym. Sci., Polym. Lett. Ed.* **1980**, *18*, 585.
(18) Scott, R. S. *J. Chem. Phys.* **1949**, *17*, 279.
(19) Hashimoto, T.; Todo, A.; Itoi, H.; Kawai, H. *Macromolecules* **1977**, *10*, 377.
(20) Hashimoto, T.; Shibayama, M.; Kawai, H. *Macromolecules* **1980**, *13*, 1237.
(21) Hashimoto, T.; Fujimura, M.; Kawai, H. *Macromolecules* **1980**, *13*, 1660.
(22) Crank, J. "Mathematics of Diffusion", 2nd ed.; Oxford University Press: New York, 1975.
(23) DiMarzio, E. A.; Guttman, C. M.; Hoffman, J. D. *Faraday Discuss. Chem. Soc.* **1979**, *68*, 210.
(24) Klein, J. *Faraday Discuss. Chem. Soc.* **1979**, *68*, 198.
(25) Tsukahara, Y.; Nakamura, N.; Hashimoto, T.; Kawai, H.; Nagaya, T.; Sugiura, Y.; Tsuge, S. *Polym. J.* **1980**, *12*, 455.
(26) Shibayama, M.; Fujimura, M.; Saijo, K.; Suehiro, S.; Hashimoto, T.; Kawai, H. *Polym. Prepr. Jpn.* **1978**, *27*, 1652. Hashimoto, T.; Suehiro, S.; Shibayama, M.; Saijo, K.; Kawai, H. *Polym. J.*, in press.
(27) Helfand, E.; Wasserman, Z. R. *Macromolecules* **1976**, *9*, 879.
(28) Hashimoto, T.; Nakamura, N.; Shibayama, M.; Izumi, A.; Kawai, H. *J. Macromol. Sci., Phys.* **1980**, *B17* (3), 389.
(29) Tsukahara, Y.; Hashimoto, T.; Kawai, H., to be submitted.
(30) Hashimoto, T.; Shibayama, M.; Kawai, H., to be submitted.
(31) Gouinlock, E. V.; Porter, R. S. *Polym. Eng. Sci.* **1971**, *17*, 535.
(32) Chung, C. I.; Lin, M. I. *J. Polym. Sci., Polym. Phys. Ed.* **1978**, *16*, 545.
(33) Arnold, K. R.; Meier, D. J. *J. Appl. Polym. Sci.* **1970**, *14*, 427.
(34) The effect of the nonvanishing thermodynamic interaction parameter χ between A and B polymers on the diffusion of polymer molecules involved in the phase transition in polymer blends is clarified from the theory by de Gennes.[36] For nonvanishing χ, the diffusion constant D_c in eq 37 should be replaced by an effective diffusion constant $D_{c,app}$, $D_{c,app} = D_c[1 - 2\chi Z\phi_A\phi_B]$, where $Z = Z_A = Z_B$ (assumed to have identical degrees of polymerization for A and B) and ϕ_K is the fraction of K polymer in the blend. Thus the value of χZ must be known in order to estimate the absolute value of D_c from the measured value $D_{c,app}$.
(35) The effect of A and B polymers having different D_c's (i.e., $D_{c,A} \neq D_{c,B}$) on the diffusion is also clarified from the theory by de Gennes[36] for polymer blends. In this case D_c in eq 37 should be replaced by an effective diffusion constant $D_{c,app}$, $D_{c,app} = D_{c,A}D_{c,B}[1 - 2\chi Z\phi_A\phi_B]/[D_{c,A}\phi_A + D_{c,B}\phi_B]$.
(36) de Gennes, P. G. *J. Chem. Phys.* **1980**, *72*, 4756.

Cholesteric Liquid Crystalline Phases Based on (Acetoxypropyl)cellulose

So-Lan Tseng, Agostino Valente, and Derek G. Gray*

Pulp and Paper Research Institute of Canada and Department of Chemistry, McGill University, Montreal, Quebec H3A 2A7, Canada. *Received November 13, 1980*

ABSTRACT: (Acetoxypropyl)cellulose ($\bar{M}_w$ = 140 000) was prepared by acetylation of (hydroxypropyl)cellulose. The polymer formed a thermotropic cholesteric phase which reflected visible light in the 85–125 °C temperature range. Solutions of (acetoxypropyl)cellulose in acetone containing more than 50 wt % polymer formed a liquid crystalline mesophase. The mesophase birefringence, reflectance, and optical rotatory dispersion were measured as a function of polymer concentration; the results confirmed the cholesteric nature of the mesophase.

Introduction

The (hydroxypropyl)cellulose–water system[1-7] forms the first reported liquid crystalline mesophase based on cellulose. (Hydroxypropyl)cellulose (HPC) also forms mesophases in organic solvents,[5,8] and there is evidence that a broad range of other cellulose derivatives[9-11] and cellulose itself[12] form anisotropic solutions at high concentrations in appropriate solvents. Interest has centered on the production of high-modulus fibers from anisotropic solutions,[9,12] but the cholesteric properties[1,3,10] of these materials may also prove useful. Numerous polymers containing cholesteryl derivatives have been synthesized,[13] but we are unaware of any reports that these display the unique optical properties associated with the cholesteric liquid crystalline state.[14] We feel that the chiral and relatively stiff molecular structure of cellulose, nature's most abundant polymer, may provide an ideal substrate for preparing novel cholesteric materials. This paper describes a new[15] cellulose derivative, (acetoxypropyl)cellulose (APC) (Figure 1), which readily forms cholesteric liquid crystalline solutions with organic solvents; the pitch of the helicoidal structure in these solutions may be varied over a wide range by changing the polymer concentration. The polymer also forms a thermotropic cholesteric phase.

Experimental Section

Preparation of Polymer. (Acetoxypropyl)cellulose was readily prepared by the acetylation of (hydroxypropyl)cellulose. (Hydroxypropyl)cellulose (Aldrich, nominal MW = 100 000) (100 g) was dissolved in 300 mL of pyridine, and 370 mL of acetic anhydride was added to the solution. After stirring overnight, the solution was refluxed briefly, allowed to cool, and poured into

* To whom correspondence should be addressed at McGill University.

0024-9297/81/2214-0715$01.25/0